International Journal of Multiphase Flow 122 (2020) 103139

Contents lists available at ScienceDirect

International Journal of Multiphase Flow

journal homepage: www.elsevier.com/locate/ijmulflow

Dimensional analysis and scaling in two-phase gas–liquid stratified pipe flow–Methodology evaluation

Raheleh Farokhpoor[a,*], Lan Liu[a], Morten Langsholt[a], Karin Hald[a], Joar Amundsen[a], Chris Lawrence[b]

[a] IFE, Institute for Energy Technology, Norway
[b] Schlumberger Software Technology, Oslo Technology Centre, Norway

ARTICLE INFO

Article history:
Received 10 July 2019
Revised 27 September 2019
Accepted 8 October 2019
Available online 11 October 2019

Keywords:
Multiphase flow
Scaling principles
Dimensionless analysis
Experimental study

ABSTRACT

Multiphase flow models are validated by comparison with a relatively good supply of high-quality laboratory data, and a relatively sparse supply of field data, which tends to have poorer quality. One of the principal challenges for multiphase flow models, in terms of uncertainty, is the difference in scale and some of the fluid properties between field and laboratory conditions. Therefore, the models may become unreliable when they are applied to conditions that are very different from those in the laboratory.

IFE (Institute for Energy Technology) has recently developed and demonstrated scale-up rules for the most basic multiphase pipe flows. The objective of the work presented in this paper was to select appropriate data from our existing database and design new, scaled laboratory experiments, well-suited to demonstrate (or test) the scaling rules by comparing the results. The data include fluid properties, pipe configurations and flow rates. Besides the observed flow pattern, liquid holdup and pressure gradient are the two main parameters for comparison.

IFE's CO_2 Flow Loop with a test section inner diameter (ID) of 44 mm, operates for two-phase flows over a large range of pressures and temperatures on the equilibrium line of pure CO_2. In order to verify scale-up principles, series of experiments were conducted according to the scaling rules to simulate similar conditions. The experiments were performed with gas–liquid two-phase CO_2 for fully-developed, steady-state flow, in a horizontal or near-horizontal pipe. The flow regimes include stratified and annular flows. The experimental results showed that measurements of liquid holdup, and pressure gradient in the CO_2 Flow Loop are in excellent agreement with appropriately scaled data from the larger-scale facilities. The results also confirm that the gas-to-liquid density ratio plays an important role. The experiments provide valuable data sets for verifying scaling laws, which are lacking in the literature.

1. Introduction

There has always been a difficulty in comparing laboratory and field data for multiphase flow. The obvious reason for this is the difference in scale. Typical field data come from pipelines with up to 1.2 m in diameter and 120 kg/m^3 and more in gas density whereas typical laboratory pipe diameters are 10 cm or less, with just a few test facilities having larger diameters (0.2–0.3 m). Models and correlations are usually developed, and partly also validated, using laboratory data. The majority of laboratories use low-density gases (e.g. air at atmospheric pressure); only a few have the possibility of using denser gases (e.g. SF_6 at 8 bara and ~50 kg/m^3 at IFE (Institute for Energy Technology)) or higher pressures (e.g. nitrogen at 90 bara and ~100 kg/m^3 at SINTEF). It is important to validate the applicability of the models with experimental results obtained for conditions similar to those experienced in field situations.

In a recent study by (AlSarkhi, et al., 2016), a model was proposed to scale up or down the pressure drop and the liquid holdup based on dimensional analysis. In this study, the pressure coefficient (so-called Euler Number) and Reynolds number of the gas phase were used to predict the pressure gradients at high-pressure conditions. The model was validated and showed good agreement with new experiments from the TUFFP (Tulsa Fluid Flow Project) high pressure facility for annular and stratified flow regimes. In another study by the same authors, (AlSarkhi, et al., 2016), a new dimensionless number (the Slippage Number) for gas–liquid flow in pipes, being a function of the Froude number was proposed. According to this study, the liquid holdup data for a wide range of

* Corresponding author.
E-mail address: raheleh.farokhpoor@gmail.com (R. Farokhpoor).

https://doi.org/10.1016/j.ijmultiphaseflow.2019.103139

Nomenclature

ρ_G, ρ_L, r_ρ	gas and liquid density, density ratio kg/m^3, [-]
μ_G, μ_L	gas and liquid viscosity mPa·s
U_{SG}, U_{SL}	gas and liquid superficial velocity m/s
σ_{GL}	gas–liquid interfacial tension mN/m
D, ε	pipe diameter (inner) and roughness mm
θ	pipe inclination angle degree, °
Fr_G, Fr_L	gas and liquid Froude number dimensionless
Re_{SG}, Re_{SL}	gas and Liquid superficial Reynolds number dimensionless
|dp/dx|	total pressure gradient Pa/m
h, H_L	chordal "holdup" and cross-sectional holdup fraction

fluids and flow conditions can be correlated with a single curve using the Slippage Number.

Statistical analysis done by (Hasan et al., 2007) showed that incorrect prediction of the flow pattern at high pressure will result in erroneous prediction of pressure drop and liquid holdup. (Abduvayt et al., 2003) performed experimental and modelling studies at high pressure conditions (20 bar) for nitrogen–water two-phase flow in a pipe with inner diameter of 106 cm. The results showed that the stratified flow region extended to higher liquid flow rates than at lower pressures. It was suggested that the mechanistic model developed for low pressures should be modified for high-pressure conditions to predict better the experimental data.

Extending dimensional analysis to multiphase flow has had limited success because the number of dimensionless groups is large, and parameters can be combined in unlimited ways to produce equally valid dimensionless groups. Scale-up using multiphase flow models has been dubious due to poor, or unknown, extrapolation properties of correlation-based models. This may change in the future with the implementation of more mechanistic models.

There are many methods of dimensional analysis, and popular methods of dimensional analysis include Rayleigh's method, Buckingham's Pi theorem, the matrix method, and the method of synthesis. All of these methods are described in (Sharp, 1981). In 1914, (Buckingham, 1914) established the Pi theorem for describing dimensionless parameters. The theorem postulates that if a physical process satisfies the principle of dimensional homogeneity and involves n relevant variables and m independent dimensions, then it can be reduced to a relationship between n and m dimensionless parameters. It is common to distinguish between three levels of similarity:

1. Geometrical similarity is satisfied if all body dimensions in all three coordinates in the model and prototype have the same length-scale ratio.
2. Kinematic similarity requires that the model and prototype have the same length-scale ratio and the same time-scale ratio (Langhaar, 1951), i.e. that the velocities are scaled accordingly.
3. Dynamic similarity exists when the model and the prototype have the same length-scale ratio, time-scale ratio, and force-scale (or mass-scale) ratio.

The paper focuses on hydrodynamic effects in two-phase flow, so our dimensional analysis does not take into account heat transfer effects. In the long-distance transport of oil and gas, the heat transfer does not strongly influence the hydrodynamics. However, the temperature and pressure do influence the fluid properties (density, viscosity and surface tension), which are included in our analysis.

For fully-developed, steady-state, gas–liquid, two-phase, stratified or stratified wavy flow in an inclined pipe, the 11 relevant variables that we consider are

1. Pipe diameter, inclination, and roughness (3 variables): D, θ, ε
2. Density and viscosity of liquid and gas (4 variables): ρ_G, ρ_L, μ_G, μ_L
3. Superficial velocity of gas and liquid (2 variables): U_{SG}, U_{SL}
4. Gravity and interfacial tension (2 variables): g, σ_{GL}

In some flow conditions, other variables may be important, including wall wetting and other surface chemical properties, but these are not considered here.

According to Buckingham's Pi theorem, the number of nondimensional parameters is equal to the number of relevant variables minus the number of independent dimensions (time, length, and mass), giving $11 - 3 = 8$ dimensionless parameters for scaling analysis. For a perfect scaling, all 8 dimensionless parameters should be identical for the two flows being compared. However, matching even half of these 8 dimensionless parameters can be difficult due to operational limitations of the flow loops. The challenge is to determine which parameters are significant and which, if any, can be safely neglected.

2. Scaling principles and procedure

IFE and its project partners have recently made significant progress in building mechanistic models for multiphase flow. Although these models are still not exact, their accuracy against available, relevant data is greatly improved. The physical basis of the models means that they possess inherent scaling properties, which have been demonstrated through comparison with a wide range of data from different laboratories and field sources (Lawrence et al., 2012; Hald et al., 2013).

To obtain well-scaled input parameters for the experiments, the following dimensionless parameters are considered:

1. The inclination angle θ is an important parameter with respect to geometrical similitude.
2. The density ratio $r_\rho = \frac{\rho_G}{\rho_L}$.
3. The most important parameter to preserve dynamic similarity in hydraulic modelling of multiphase flows influenced by gravity is the Froude number. In this work, we have assumed similarity through the squared Froude number $Fr_{SG}^2 = \frac{\rho_G U_{SG}^2}{(\rho_L - \rho_G) gD} = \frac{r_\rho U_{SG}^2}{(1-r_\rho) gD}$ to determine the target value of U_{SG}.
4. The liquid-to-gas superficial velocity ratio U_{SL}/U_{SG} is used to obtain kinematic similarity. Together with 3, this determines the target value of U_{SL}.
5. The Reynolds number is always relevant, with or without multiple phases. The inverse Reynolds numbers $Re_{SL}^{-1} = \frac{\mu_L}{\rho_L U_{SL} D}$ and $Re_{SG}^{-1} = \frac{\mu_G}{\rho_G U_{SG} D}$ can be used to determine the target values of the viscosities μ_G and μ_L.
6. Matching the inverse Weber number $We^{-1} = \frac{\sigma_{GL}}{\rho_G U_{SG}^2 D}$ is used to determine the target value of the surface tension σ_{GL}.
7. The final parameter is the roughness to diameter ratio, ε/D.

In this study, the density ratio is prioritised for matching. For this purpose, two-phase gas–liquid CO_2 at different pressures and temperatures is used. With the experimental limitations, it is extremely difficult to find a fluid system which meets all the scaling requirements. With judgement derived from modelling experience, and preliminary studies, the last four dimensionless parameters, items 5, 6 and 7 in the numbered list above, are considered to be less important, and are not matched. The two dimensionless output parameters for scaling comparison are:

Table 1a
Experimental conditions in earlier work at Tiller and IFE flow loops.

Experiment	D mm	Fluids [–]	Pipe angle °	Pressure bara	U_{SL} m/s	U_{SG} m/s
Tiller	289	N_2–Naphtha	5.0	45	0.05, 0.15	3.0–5.0
LS1			5.0	90	0.05, 0.15	3.0–5.2
IFE WFL1	99	SF_6–Exxsol D80	5.0	7	0.03, 0.095	2.0–5.0
Tiller LS2	189	N_2–Naphtha	1.0	21	0.01, 0.06, 0.2	0.5–12.0
IFE WFL2	99	SF_6–Exxsol D80	1.0	4	0.007, 0.04, 0.15	0.04–9.0

Table 1b
Fluid properties used in Experiments at Tiller and IFE flow loops.

Experiment	Density ratio	Original Fluid properties in each Lab.			Scaled values at IFE WFL ($D = 99$ mm)		
	$\rho_G/\ \rho_L$ [–]	μ_L mPa·s	μ_G mPa·s	σ_{GL} mN/m	μ_L mPa·s	μ_G mPa·s	σ_{GL} mN/m
Tiller	0.078	0.256	0.018	13.3	0.064	0.004	2.0
LS1	0.155	0.258	0.02	10.9	0.068	0.003	1.8
IFE WFL1	0.057	1.8	0.015	21			
Tiller LS2	0.035	0.312	0.10	14.4	0.14	0.005	4.8
IFE WFL2	0.035	1.8	0.015	22.6			

1. Total pressure gradient per unit length in the form of $\frac{D}{\rho_G U_{SG}^2}(\frac{dp}{dx}+\rho_G\ g\ \sin\theta)$;
2. Liquid holdup H_L

In the context of our dimensional analysis, the flow pattern is also an output parameter.

The objective of this study was to select appropriate data from our existing data sets and design scaled-down laboratory experiments for the CO_2 flow loop at IFE, to reproduce the same (scaled) flow conditions. This demonstrates a procedure that could be used to design laboratory experiments relevant to full scale field conditions.

It is straightforward to evaluate the scale-up rules by comparing results. The aim is to generate data for comparison and verification of the scale-up principles in the simplest cases. For this purpose, the steps described here have been undertaken:

1. High-quality laboratory data from medium- and large-scale pipes for two-phase, gas–liquid stratified flow are chosen for scaling comparisons, listed in Table 2.
2. By assuming equal dimensionless numbers (items 1–4 in the dimensionless parameter list above), the fluid flow properties (flow rates, pipe inclination and density ratios) were scaled to design experiments with CO2 as the working fluid in a pipe with ID = 44 mm.
3. Finally, measurements of liquid holdup and a dimensionless form of the pressure gradient were compared, as were the observed flow patterns.

3. Earlier study

In 2012, a small experimental campaign was carried out in IFE's Well Flow Loop, (Lawrence et al., 2012), to verify the scaling rules with respect to experiments from SINTEF's Large Scale Loop at Tiller. The objective of this experimental campaign was to generate some data for comparison and verification of the scale-up principles in the simplest cases. The test matrices for the two datasets are given in Table 1a: Tiller data from 1993 to 1995 (Hedne, 1996; Heggum, 1993) named as Tiller LS1 with pipe diameter of 289 mm and 5.0° upward inclination and Tiller LS2 with pipe diameter of 189 mm and 1.0° upward inclination. The fluids were naphtha and nitrogen at nominal pressures of 21, 45 and 90 bara, with the density ratios of 0.035, 0.078 and 0.15 respectively. Subsets of the data with U_{SL} values in the range from 0.01 m/s to 0.2 m/s, in stratified wavy flow, were identified.

Table 2
Overview of original datasets from Tiller.

Dataset	Dataset 1	Dataset 2
Year	1986	1995
Pipe D, mm	194	289
Pressure, bara	45, 65 and 90	45 and 90
Fluids, two phase gas–liquid	N_2–Naphtha	N_2–Naphtha, N_2–Diesel
Inclination, °	1.0, 0.0, −1.0	5.0
Original U_{SL}, m/s	0.06–1.3	0.1–0.3
Original U_{SG}, m/s	0.5–12.0	1.0–5.0

Correspondingly, we have the IFE Well Flow Loop (Lawrence et al., 2012) experiments with 99-mm pipe diameter and the same inclinations. In IFE WFL1 experiments, SF_6 and Exxsol D80 at 7 bara with density ratio of 0.057 were used to simulate Tiller LS1 experiments with density ratios of 0.078 and 0.15. Due to experimental limitations, the density ratio was not matched with Tiller LS1 experiments; these experiments were intended to assess the importance of the density ratio. In IFE WFL2, with a similar fluid system at nominal pressure of 4 bara, the density ratio of 0.035 was closely matched with Tiller LS2. The superficial velocity values, U_{SL} and U_{SG}, used in the IFE experiments given in Table 1a, were designed to match the Tiller experiments based on the scaling rules described in the previous section.

Fluid properties including the gas and liquid viscosities and gas–liquid interfacial tension values are given in Table 1b. In the last three columns, the viscosity (and surface tension) values given for the Tiller flow loop are hypothetical values that would be required to achieve a perfect scaling. These hypothetical values are obtained from the actual fluid properties of the Tiller experiments by scaling down to the IFE Well Flow Loop scale (ID = 99 mm) using Reynolds number and Weber number.

In Fig. 1, measured total pressure gradient (magnitude) and liquid holdup for Tiller and IFE experiments are compared. The aim was to replicate the Tiller experiments. Here, the Tiller results have been scaled down to IFE WFL scale (with pipe diameter of 99 mm). The error lines in the two panels have a different appearance. In the upper panel, the error in the pressure drop measurement is an absolute error for smaller measurements, and a relative error for larger measurements, so the error lines diverge for larger value. In the lower panel, the error in the holdup measurement is an absolute error, so the error lines are parallel.

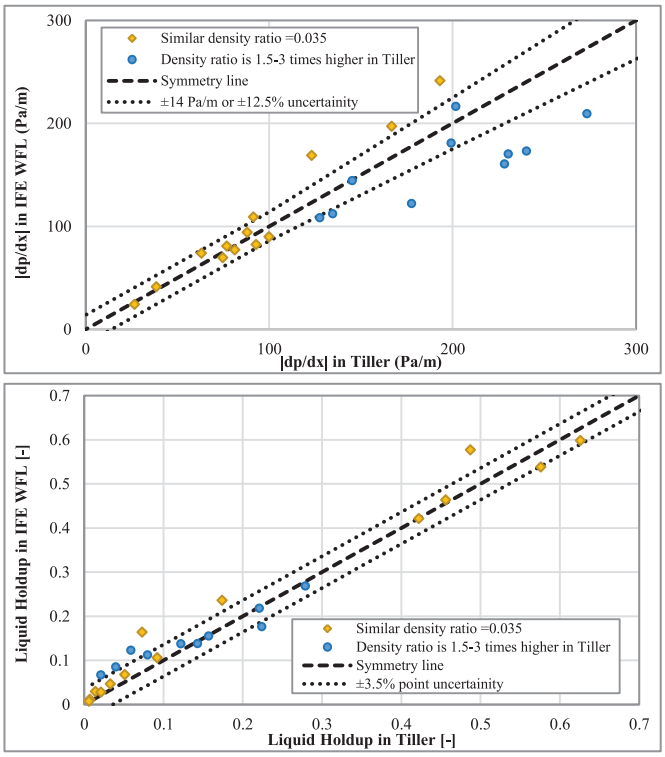

Fig. 1. Experimental results for the inclination from earlier works at Tiller and IFE (pressure gradient in upper graph and liquid holdup in lower graph).

As can be seen in Fig. 1, for experiments with the density ratio of 0.35 and pipe with 1.0° upward inclination, there is very good agreement in both pressure gradient and liquid holdup. In IFE WFL1 experiments, where the density ratio is 1.5–3 times smaller than in the Tiller experiments and pipe inclination is higher, 5.0° upward, the pressure gradients are overestimated, but there is a good match in the liquid holdup. We believe that the large difference in the density ratio is the main reason for the deviations found in the pressure gradients.

4. Available datasets

As we mentioned earlier, the aim is to generate some data for comparison and verification of the scale-up principles in the simplest cases. For this purpose, we have selected 38 subsets, a total of 145 experiments, which are categorized as Dataset 1 and Dataset 2 in Table 2. 29 subsets are from Dataset 1 (Hedne, 1988; Linga and Hedne, 1987; Linga and Østvang, D., 1985), where the pipe diameter is 194 mm, the fluids are nitrogen and naphtha at nominal pressures of 45, 65, and 90 bara. The pipe inclinations include horizontal, 1.0° upward, and 1.0° downward inclinations. Liquid superficial velocity ranges from 0.06 m/s to 1.3 m/s. For a constant U_{SL}, gas superficial velocity varies from 0.5 m/s to a maximum of 12 m/s in each of the subsets.

Dataset 2 consists of nine subsets of experiments with pipe diameter of 289 mm and 5.0° upward inclination. Two fluid systems were used; naphtha and nitrogen at nominal pressures of 45 bara and 90 bara, and diesel and nitrogen at nominal pressure of 45 bara. For each fluid system, at a certain pressure, three subsets of the data with U_{SL} values close to 0.1, 0.15 and 0.3 m/s and U_{SG} ranging from 1.0 to 5.0 m/s were identified. The flow regime changes from stratified wavy at low U_{SG} to dispersed flow at high U_{SG}.

5. The CO_2 flow loop

A CO_2 test rig has been constructed at IFE, referred to as the CO_2 Flow Loop. The test section is a stainless steel pipe with diameter of 44 mm and 5.0 μm wall roughness. This pipe, 13-m long (~300 diameters) is mounted on an inclinable rigid steel beam. The beam can be tilted to roughly ±10° inclination. The test section has the following instruments and equipment (Fig. 2):

- Three Fuji dP-transducers (TS.dP1, TS.dP2 and TS.dP3)
- Three absolute pressure transducers (TS.P1–P3) and three temperature transducers (TS.T3–T5) and four temperature sensors at the inlet and outlet of the test section (two at each end).
- One clamp-on narrow beam gamma densitometer (TS. γ)
- One visualization section with two sight glasses (TS.SG)
- Heat exchanger made from longitudinally attached copper tubing for controlling the temperature of the test section

To keep the fluid in the entire test rig as close as possible to a uniform temperature, all the parts of the cooling system run as an integrated system with one set-point. This works very smoothly, and temperatures in the range of −10°C–+40°C can normally be obtained. The data acquisition system for the CO_2-loop is based on National Instrument's (NI) Compact FieldPoint data logging modules (PLCs) and LabVIEW software. The gas and liquid mass flow rates are measured using two Rheonik RHM 20 Coriolis meters, which are specified for measuring gas and liquid phase CO_2, respectively

A narrow-beam gamma densitometer is used to measure the chordal liquid fraction, h/D, across a diameter of the pipe in a vertical plane. The gamma densitometer includes an 11 GBq ^{241}Am gamma source, a source holder, a detector, digiBASE-E multichannel analyser from ORTEC, and a collimator. A PC with a LabVIEW application communicates with the base, and the data are logged using in-house software.

The holdup measurements compared in the paper come from two different types of instrument. The broad beam gamma densitometer on the IFE Well flow loop gives a direct measurement of holdup (within a certain margin of error). The narrow beam gamma densitometers in our experiments (IFE's CO_2 flow loop) and at SINTEF give a measurement of the liquid height only. In order to compare these measurements, a conversion is necessary, and the formula based on a flat interface is the simplest and most robust way to do this. The use of this conversion has been assessed many times at SINTEF by comparing with direct holdup measurements obtained using quick closing valves. The conversion introduces an additional uncertainty which is included in the stated uncertainty range of the measurements. For the narrow beam instruments, the pipe cross-sectional holdup H_L is estimated assuming a flat gas–liquid interface:

$$H_L = \frac{A_L}{A} = \frac{1}{2\pi}(2\delta - \sin 2\delta), \quad h/D = \frac{1}{2}(1 - \cos\delta) \tag{1}$$

where A is the pipe cross sectional area, A_L is the cross section of the pipe filled with liquid and δ is the wetted half-angle, illustrated in Fig. 3.

The CO_2 flow loop can operate in two-phase flow over the range of −10 °C–+30 °C (the critical point), corresponding to pressures from 26.5 to 73.7 bar, which allows access to gas–liquid density ratios in the range 0.07–1.0. It is difficult to control experiments near the critical point, but the operating temperature can be increased above the critical point and up to +40 °C where CO_2 is in supercritical phase. The gas–liquid phase boundary for CO_2 is shown in Fig. 4, which also shows the gas–liquid density ratio at the phase boundary as a function of the temperature.

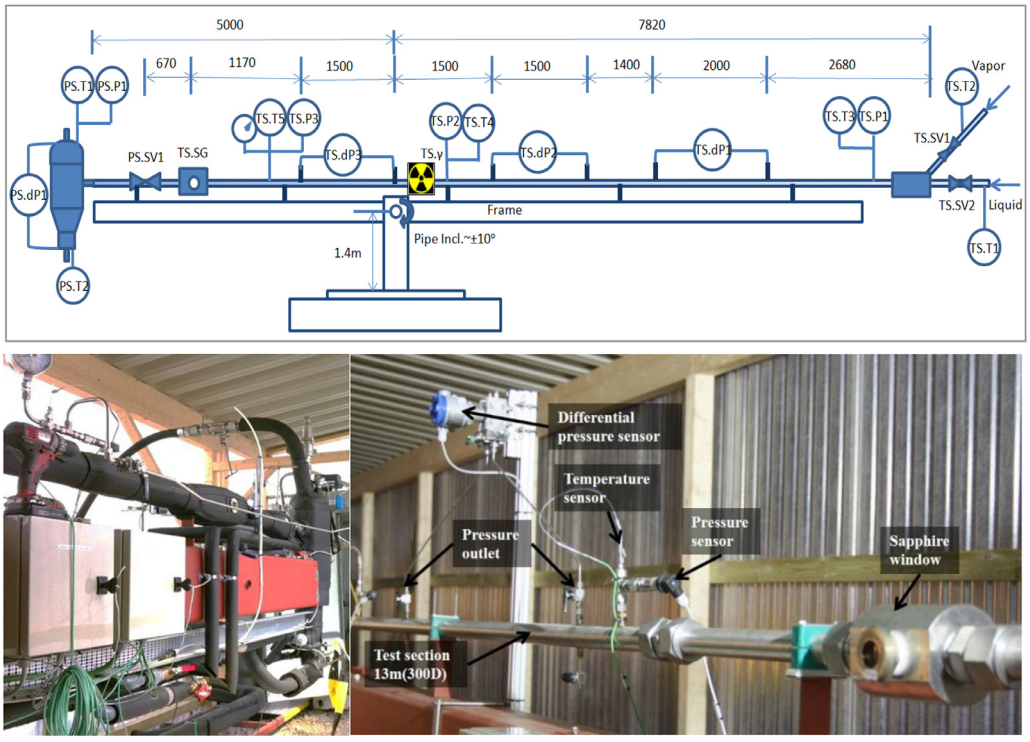

Fig. 2. Top: Schematic diagram of the test section of the CO_2 flow loop. Bottom: part of test section with and without insulating materials.

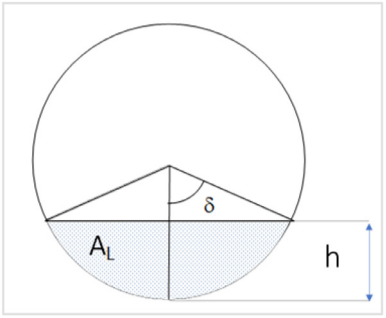

Fig. 3. A schematic diagram of the cross-section geometry in two-phase stratified flow.

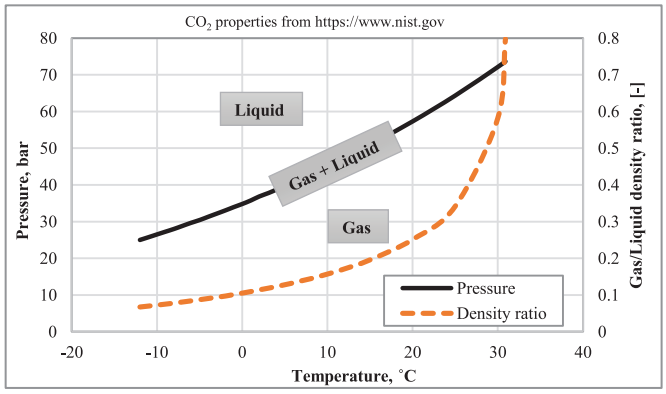

Fig. 4. The phase diagram for CO_2 for the CO_2 flow loop operating conditions and the gas–liquid density ratio as a function of temperature.

6. Experimental procedure

1. The pipe inclination was adjusted and fixed.
2. Prior to the experiments, the test section was flooded with gaseous CO_2 and the sight-glass was used to make sure that there was no liquid left in the test section.
3. The impulse lines for the dp-transducers were bled off and the signal/output was zeroed. The zero point of the transducers was set at static conditions with single-phase gas in the pipe and with the test section at the desired inclination. Therefore, to convert the measured differential pressure (magnitude) to the actual total pressure gradient, the following expression should be used:

$$dp/dx = dp/dx_{measured} + \rho_G g \sin\theta \quad (2)$$

where θ is the pipe inclination.
4. The gamma densitometer was calibrated daily or when the fluid temperature changed significantly (by say, 2–3 °C). Count rates were measured for both pure vapour and pure liquid phases and given as input to the LabVIEW programme, as this is required input to the holdup algorithm.
5. For a fixed U_{SL}, U_{SG}-sweeps were performed by starting with a high value of U_{SG} and then step-wise reducing U_{SG} according to the planned test matrix. (In this manner, reaching steady-state flow is faster than the other way around, i.e. stepping up in U_{SG}). For each U_{SG}, holdup and pressure gradients were measured.
6. To match the density ratio, we used pure CO_2 at different temperatures (and thus pressures) in the range from −12 °C–+10 °C, depending on the experiment. The temperature at the inlet of the test section was used to calculate the thermodynamic properties of liquid and gas CO_2.

7. Measurement uncertainty

All measurements are subject to degrees of uncertainty, which for the CO_2 Flow Loop have been estimated by combining Type B standard uncertainties (instrument accuracy, repeatability, linearity, ambient conditions, drift, offset, etc.) and the Type A standard

Table 3
Estimated measurement uncertainties in input and measured data.

Parameter	Uncertainty in CO_2 loop	Uncertainty in Tiller loop
Pipe inclination	±0.05°	±0.1°
Pipe diameter	±0.4 mm	±1%
Absolute pressure	±0.1 bara	Not available
Temperature	±1.0° C	Not available
Liquid holdup	±0.02–0.03 (absolute)	±0.01–0.02
Liquid superficial velocity	±2–7%	±3%
Gas superficial velocity	±2–5%	±1%
Pressure gradient (>100 Pa/m)	±5–10%	±7.5%
Pressure gradient (<100 Pa/m)	±10 Pa/m	±10 Pa/m
Liquid density	±0.5–1.0%	±0.5%
Gas density	±2.5–3.5%	±5%

uncertainty, which is based on statistical treatment of repeated measurements. The best estimated total uncertainties are given in Table 3.

The uncertainty in the holdup measurements is generally of the order ±0.02–0.03 (absolute error). The uncertainty in the pressure gradient is generally in the range ±5%–10% of reading (relative error). In some experiments where the pipe has 1° or 5° downward inclination, the pressure gradient reaches to zero at low U_{SG} so the error in is assumed to have a lower limit which is the value specified by the instrument manufacturer, 10 Pa/m (absolute error). Because the fluid mass flow rates are measured, rather than the volumetric flow rates, the uncertainties in the pipe diameter and gas and liquid densities contribute to the resulting uncertainties in the gas and liquid superficial velocities. Gas and liquid densities are taken from National Institute of Standards and Technology (NIST) (US Department of Commerce, n.d.), and the uncertainty in densities given in Table 3 is mostly due to variations in the temperature.

For the output data (flow regimes, H_L, |dp/dx|) in this study, minor changes in the pipe wall roughness, liquid and gas viscosity, and interfacial tension are not expected to have a strong influence on the results. We, therefore, anticipate that the measured values are relatively insensitive to uncertainties in these parameters. The effect of the uncertainty in the pipe inclination (±0.05°) on the measurements is also very small.

8. Experimental results for dataset 1

In this section, the results from the CO_2 Flow Loop experiments and subsequent data analysis are presented. Firstly, we compared Tiller Dataset 1 experiments with our experiments in the CO_2 Flow Loop. Exp 1–Exp 29 correspond to the 29 subsets from Dataset 1, with the experimental conditions listed in Table 4. As explained earlier in this paper, the aim was to simulate Tiller experiments, with matching density ratio being prioritized. Therefore, in Exp 1–Exp 29, two phase CO_2 at different temperatures, −7, 0 and 10° C, was used to match the density ratio in corresponding experiments Tiller 1–Tiller 29 (see Table 4). The detailed results are given in Table 6 in the Appendix.

Gas and liquid superficial velocities in Tiller experiments were scaled down to the CO_2 flow loop according to the scaling procedure explained earlier. In Table 4, the U_{SL} values used in the Tiller experiments and the scaled values used in the CO_2 flow loop are given. The liquid viscosity and gas–liquid interfacial tension are listed for pure CO_2 at the given temperature. The values of these properties for the Tiller experiments are scaled down to CO_2 flow loop scale (with pipe diameter of 44 mm), using liquid Reynolds number and Weber number (as in Table 1b), and the target values are given in Table 4. In all 29 experiments, for each U_{SL}, U_{SG} is slowly decreased in quite small steps from approximately 5 m/s–0.5 m/s.

Exp 1–Exp 13 were performed with a horizontal pipe for three different fluid systems representing density ratios of 0.15, 0.11 and 0.08. To match the gas-to-liquid density ratio of the fluids used in the Tiller experiments, two-phase CO_2 at temperatures of 10° C, 0.0 ℃ and −7° C was used. The liquid viscosity and gas–liquid surface tension in the CO_2 Flow Loop are significantly higher than the scaled values from the corresponding Tiller experiments. The comparison of results (below) demonstrates that this difference is not very important. Exp 14–Exp 21 correspond to the eight subsets from Dataset 1 for a pipe with 1.0° upward inclination. Tiller experiments were carried out with nitrogen and naphtha at 45 and 90 bara and 20° C. To reach similar density ratios in the CO_2 Flow Loop, two-phase, CO_2 at −7° C and 10° C was used. Lastly, Exp 22–Exp 29 include eight subsets of experiments that were conducted

Table 4
Experimental conditions and fluid properties used in CO_2 Flow Loop and Dataset 1.

Experiment	D	Pipe angle	Temp.	Press.	ρ_G/ρ_L	Original U_{SL}	Scaled down to CO_2 Flow Loop	
	mm	°	°C	bara	[–]	m/s	μ_L mPa·s	σ_{GL} mN/m
Exp 1–Exp 4	44	0.0	10	45	0.15	0.05, 0.1, 0.5, 0.8	0.083	~3
Tiller 1–Tiller 4	194	0.0	20	90	0.15	0.06, 0.1, 0.2, 1.0	0.045	0.72
Exp 5–Exp 9	44	0.0	0.0	35	0.11	0.1, 0.2, 0.3, 0.4, 0.6	0.10	~4.5
Tiller 5–Tiller 9	194	0.0	20	65	0.11	0.2, 0.4, 0.6, 0.8, 1.3	0.033	0.88
Exp 10–Exp 13	44	0.0	−7	28.8	0.081	0.03, 0.05, 0.1, 0.5	0.11	~6.0
Tiller 10–Tiller 13	194	0.0	20	45	0.082	0.06, 0.1, 0.2, 1.0	0.05	0.97
Exp 14–Exp 17	44	1.0	10	45	0.15	0.03, 0.05, 0.1, 0.5	0.083	~3
Tiller 14–Tiller 17	194	1.0	20	90	0.15	0.06, 0.1, 0.2, 1.0	0.042	0.7
Exp 18–Exp 21	44	1.0	–7	28.8	0.081	0.03, 0.05, 0.1, 0.5	0.112	~6.0
Tiller 18–Tiller 21	194	1.0	20	45	0.076	0.06, 0.1, 0.2, 1.0	0.047	0.8
Exp 22–Exp 25	44	−1.0	10	45	0.15	0.03, 0.05, 0.1, 0.5	0.08	~3
Tiller 22–Tiller 25	194	−1.0	20	90	0.15	0.06, 0.1, 0.2, 1.0	0.04	0.7
Exp 26–Exp 29	44	−1.0	–7	28.8	0.081	0.03, 0.05, 0.1, 0.5	0.112	~6.0
Tiller 26–Tiller 29	194	−1.0	20	45	0.076	0.06, 0.1, 0.2, 1.0	0.046	1.0

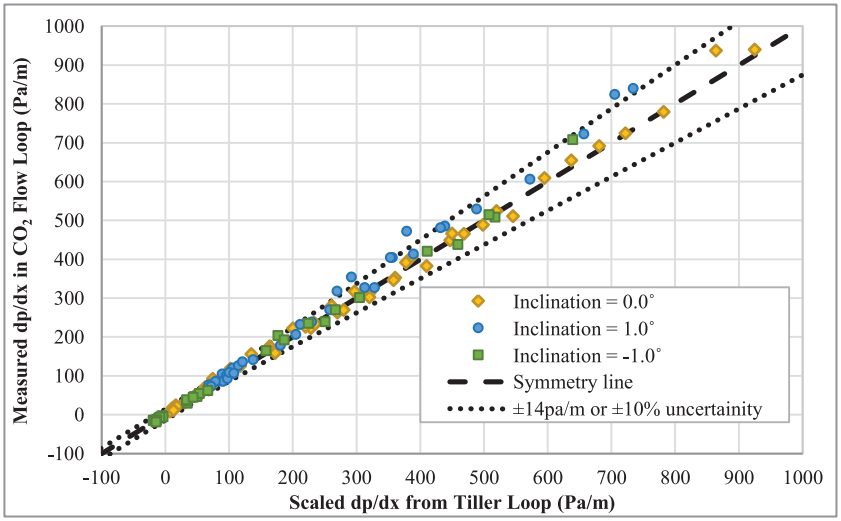

Fig. 5. Total pressure gradient in CO_2 flow loop and corresponding Tiller experiments.

using two-phase CO_2 at 10 and −7° C respectively, in a pipe with inclination of 1.0° downward.

The pressure gradient measurements obtained from the CO_2 Flow Loop experiments are compared with scaled values of the pressure gradient measurements from the Tiller experiments. The dimensionless pressure parameter in the form of $\frac{D}{\rho_G U_{SG}^2}\left(\frac{dp}{dx}+\rho_G\, g\, \sin\theta\right)$ is used to determine the expected total pressure gradient in the CO_2 Flow Loop. In Fig. 5, the scaled values of the pressure gradient (magnitude) are compared with measured values from the CO_2 Flow Loop for three different pipe inclinations.

As can be seen in Fig. 5, there is excellent agreement in the pressure gradients between the CO_2 Flow Loop and the Tiller experiments for all density ratios and all three pipe inclinations. The total pressure gradients at high gas superficial velocity ($U_{SG} > 4$ m/s), were measured slightly higher than the scaled values from the Tiller experiments. One explanation for this deviation can be that at higher U_{SG}, there is more droplet entrainment, so that effects of interfacial tension and liquid viscosity are not entirely negligible.

The uncertainty lines are the combination of uncertainties in data from the CO_2 flow loop and the Tiller loop, calculated by Eq. (3):

$$\text{Total error in } dp/dx = \left(\text{Error in } dp/dx_{CO2\ \text{Flow Loop}}{}^2 + \text{Error in } dp/dx_{\text{Tiller Loop}}{}^2\right)^{1/2} \quad (3)$$

Therefore,

1. For $dp/dx > 100$ Pa/m; uncertainty is 12.5% of reading (relative error).
2. For $dp/dx < 100$ Pa/m; uncertainty is 14 Pa/m (absolute error).

For 1.0° upward pipe inclination, both the CO_2 Flow Loop and the Tiller experiments show a similar minimum in the pressure gradients, associated with the change from gravity-dominated to friction-dominated flow. Likewise, for 1.0° downward pipe inclination, as U_{SG} decreases step by step, and for $U_{SG} < 1$ m/s, the average pressure gradient approaches zero and then the flow becomes gravity dominated. For better understanding, the total pressure gradient for three experiments in the CO_2 flow loop with horizontal pipe, and for 1.0° upward and downward pipe inclinations are shown in Fig. 6. All experiments are for two-phase CO_2 at the temperature of 10° C (density ratio of 0.15) with $U_{SL} = 0.1$ m/s. Scaled

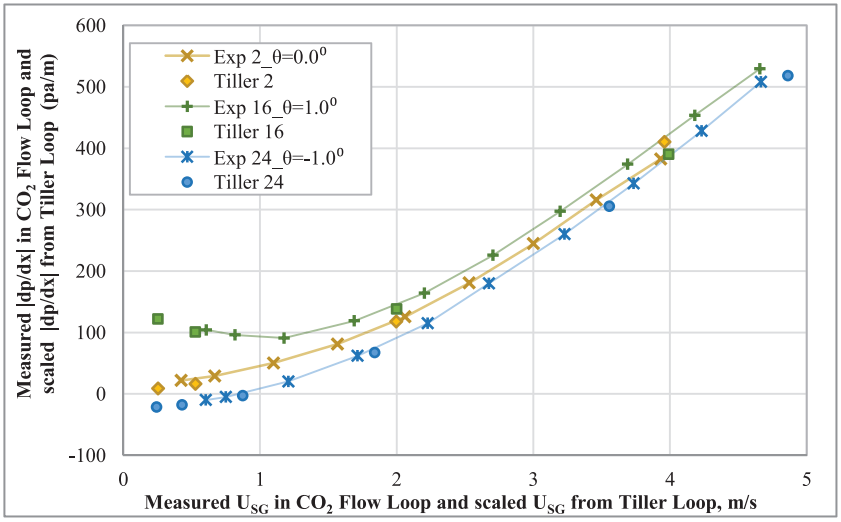

Fig. 6. Total pressure gradient measured directly in CO_2 flow loop and the scaled values from Tiller loop for three different inclinations with density ratio = 0.15 and $U_{SL} = 0.095$ m/s.

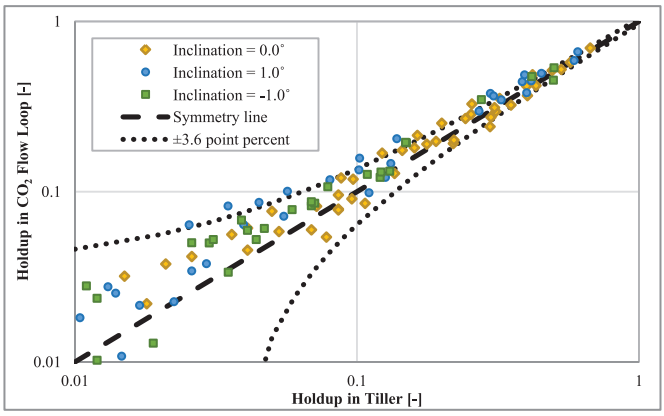

Fig. 7. Liquid holdup in CO_2 flow loop and corresponding Tiller experiments.

values from corresponding Tiller experiments are also shown in the figure.

Since liquid holdup is already dimensionless, the measured liquid holdups from the CO_2 Flow Loop are compared directly with measured values from the Tiller experiments. As exhibited in Fig. 7, the liquid holdup values match very closely with the equivalent experiments at Tiller. The combined uncertainty in liquid hold up is calculated in the same way as the one for pressure gradient by Eq. (3) and is 0.036 absolute error. Large relative deviations in the measured liquid holdup can be seen when it falls below 10%. But these differences are of similar magnitude to the combined uncertainty in the holdup measurements.

The flow pattern determination in the Tiller experiments is based on video recordings. For horizontal and near horizontal flow, gas–liquid distribution is classified into four major patterns; annular flow, stratified wavy flow, slug flow and dispersed-bubble flow. In our experiments, we use video recordings, time series of liquid holdup and the probability distribution function of the holdup to determine the flow pattern.

There are systematic trends in the flow pattern. In these experiments, for all three density ratios (0.15, 0.11 and 0.078) and all three inclinations (−1.0, 0.0 and 1.0°), for $U_{SL} > 0.38$ m/s, the flow regime is large wave flow, with the interface becoming smoother as U_{SG} reduces. For low U_{SL} (0.03, 0.05 and 0.095 m/s), the flow is mainly stratified-annular flow at high U_{SG} and stratified wavy flow at lower U_{SG}, except for the pipe with inclination of 1.0° upward and density ratio of 0.078, for which large wave flow is observed for $U_{SG} < 1$ m/s. In all 29 Tiller experiments (named Tiller 1–Tiller 29), for all density ratios and pipe inclinations, and for $U_{SL} < 0.1$ m/s, the flow is described as stratified wavy flow for the entire range of U_{SG}. For $U_{SL} < 0.2$ m/s and $U_{SG} > 3.5$ m/s, the flow pattern is identified as annular flow. The flow pattern maps for both CO_2 flow loop experiments and Tiller experiments (for all three inclinations and density ratios) are presented in Fig. 8 with scaled velocities. The lines in this figure are indications or the approximate boundaries between the different flow patterns.

The flow pattern map for CO_2 Flow Loop look different from Tiller loop. We think that the differences between the flow pattern observations in the left and right panels are caused by two main factors:

1. For the Tiller experiments, conducted in 1986, the information available to determine the flow pattern was very limited. This made it very difficult to identify the flow pattern with any degree of confidence, so it is quite possible that the reported flow pattern is not always correct.
2. Even in the best circumstances, the identification of the flow pattern represents the subjective opinion of the observer. The experiments were conducted by different researchers at different laboratories with many years in between, and this may explain the systematic differences in the reported flow patterns.

Nevertheless, the three-flow patterns, stratified-wavy, stratified-annular and large waves are rather similar with no sharp distinctions. They could all be regarded as variations of one flow pattern, e.g. wavy-stratified annular, so that the apparent large difference in observed flow patterns may not be very significant.

9. Experimental results for dataset 2

Tiller Dataset 2 from 1995 was obtained using a pipe with a diameter of 289 mm and 5.0° upward inclination. Two fluid systems were used; naphtha and nitrogen at nominal pressures of 45 bara and 90 bara, and diesel and nitrogen at nominal pressure of 45 bara. For each fluid system and specific pressure, three subsets of the data with U_{SL} values of 0.1, 0.15 and 0.3 m/s in stratified-wavy flow were identified. In Table 5, the CO_2 Flow Loop experiments and corresponding Tiller experiments are listed. The detailed results are given in Table 7 in the Appendix. As mentioned earlier, to match the Tiller experiments' density ratios, two-phase

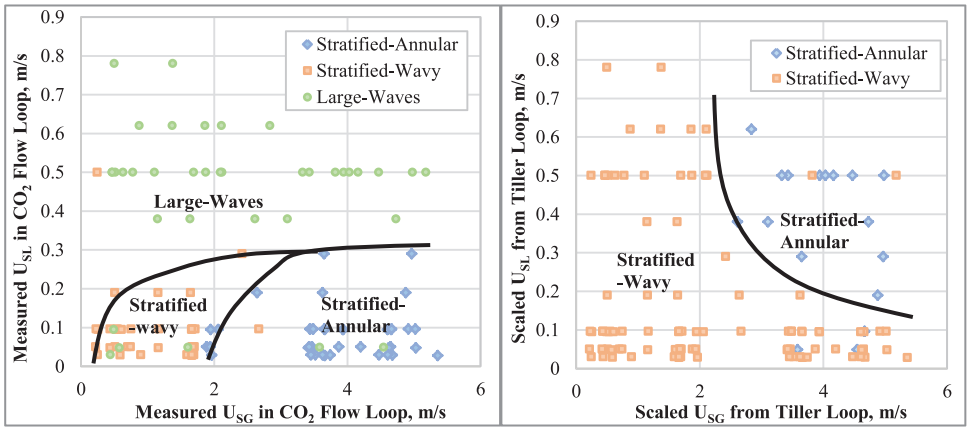

Fig. 8. Flow pattern map for CO_2 flow loop experiments (to the left) corresponding to Tiller dataset 1 (to the right).

Table 5
Experimental conditions and fluid properties used in Exp 30–Exp 38 and corresponding Tiller experiments for the pipe with inclination of 5.0° upward.

Experiment	ID	Liquid	Temp.	Press.	ρ_G/ρ_L	Original U_{SL}	Scaled down μ_L	σ_{GL}
	mm	[–]	°C	bara	[–]	m/s	mPa·s	mN/m
Exp 30–Exp 32	44	CO_2	10	45	0.15	0.04, 0.06, 0.12	0.083	~3
Tiller 30–Tiller 32	289	Naphtha	20	90	0.15	0.1, 0.15, 0.3	0.021	0.33
Exp 33–Exp 35	44	CO_2	−8	28	0.078	0.04, 0.06, 0.12	0.114	~6.0
Tiller 33–Tiller 35	289	Naphtha	20	45	0.078	0.1, 0.15, 0.3	0.022	0.45
Exp 36–Exp 38	44	CO_2	−12	25	0.067	0.04, 0.06, 0.12	0.122	~6.5
Tiller 36–Tiller 38	289	Diesel	20	45	0.06	0.1, 0.15, 0.3	0.156	0.65

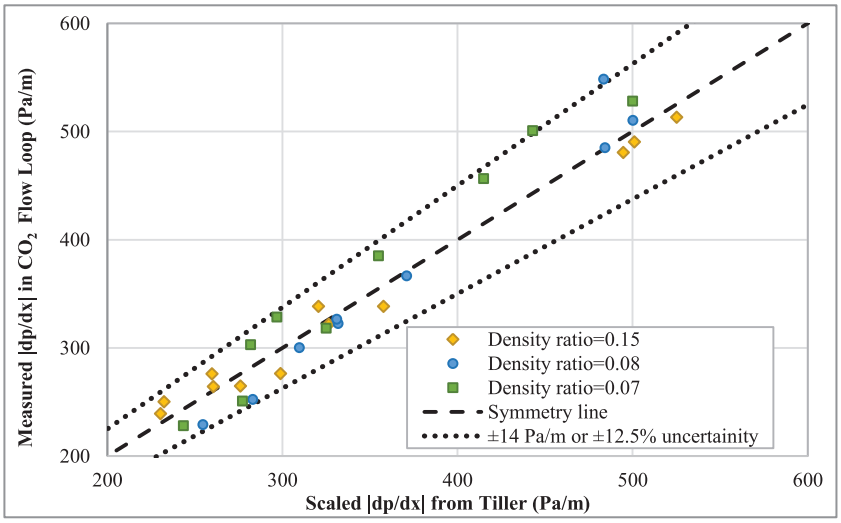

Fig. 9. Total pressure gradient in CO_2 flow loop and scaled values from the corresponding Tiller experiments for the pipe with inclination of 5.0° upward and for different density ratios.

gas–liquid CO_2 experiments at three different temperatures were used. The same procedure as explained for Dataset 1 is applied here.

Exp 30–Exp 32 are designed to replicate the three subsets of experiments from Tiller that were performed with nitrogen and naphtha at 90 bara and 20 °C temperature. At this condition, the nitrogen to naphtha density ratio is 0.15 and to match this value, two-phaseCO_2 at 10 °C was used. For Exp 33–Exp 35, two-phase gas–liquid CO_2 at −8 °C gives the density ratio of 0.078. These experiments are representative of Tiller experiments for nitrogen and naphtha at 45 bara and 20 °C temperature, as mentioned in Table 5. In Exp 33–Exp 35, CO_2 liquid viscosity and gas–liquid interfacial tension are significantly higher than the scaled values from the Tiller experiments. Again, the comparison of results (below) demonstrates that this difference is not very important. Exp 36–Exp 38 correspond to Tiller experiments for diesel and nitrogen at 45 bara. At this pressure, the nitrogen to diesel density ratio is 0.06 and with the temperature limitations in the CO_2 Flow Loop, with two-phase CO_2 at −12 °C, a density ratio of 0.067 was the lowest that could be achieved. In these experiments, for the first time, CO_2 liquid viscosity (0.122 mPa.s) is very close to the scaled value (0.156 mPa.s), but the gas–liquid surface tension is ten time higher.

The measurements of total pressure gradient (magnitude) and liquid holdup are compared in Fig. 9 and Fig. 10, with symbols indicating the density ratio. Pressure gradients are in excellent agreement with the scaled values from the Tiller experiments, with slight deviation at higher values, but still within the range of experimental uncertainty. For experiments with density ratios of 0.15 and 0.078, the liquid holdup matches very well with the Tiller experiments. For experiments with lowest density ratio (0.06), there are some discrepancies in the liquid holdups, with 10–20% higher values measured in the CO_2 Flow Loop compared to the Tiller experiments.

In these experiments, for all three density ratios (0.15, 0.078 and 0.06) and U_{SL} (0.04, 0.06 and 0.12 m/s), the flow pattern is quite similar. Stratified-annular flow was identified at high U_{SG}, changing to stratified-wavy flow and, finally, to large waves at U_{SG} values where the pressure gradient reaches its minimum. With lower density ratio, the minimum in pressure gradient occurs at slightly higher U_{SG}, which means that large waves flow pattern happens at higher U_{SG}. In the Tiller experiments, the flow pattern for experiments with density ratios of 0.15 and 0.078 was identified as stratified-wavy, except for the lowest $U_{SG} = 0.45$ m/s, where slug flow was reported. For the lowest density ratio of 0.06, slug flow was reported for a larger range of $U_{SG} < 1.2$ m/s. The flow pattern maps for the CO_2 Flow Loop and the Tiller experiments are compared in Fig. 11. Both experiments present stratified-wavy flow regime with similar boundaries. For $U_{SG} < 1.5$ m/s, the flow patterns were observed differently in two loops, but we think for the same reason as we mentioned in previous section, it is difficult to distinguish between these two flow regimes, and they can be very similar. As we explained in the previous section, the differences may be due to the limited information available about the Tiller experiments, coupled with subjective differences in flow pattern identification.

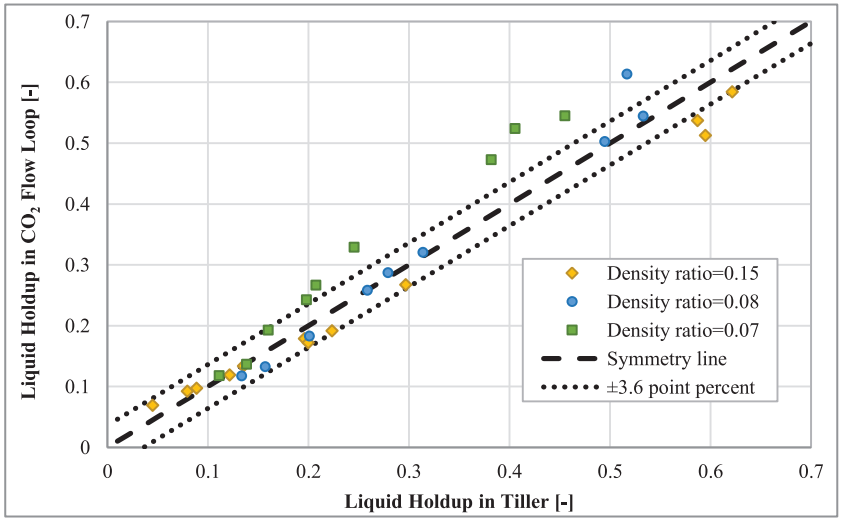

Fig. 10. Liquid holdup in the CO_2 flow loop and the corresponding Tiller experiments for the pipe with inclination of 5.0° upward and for different density ratios.

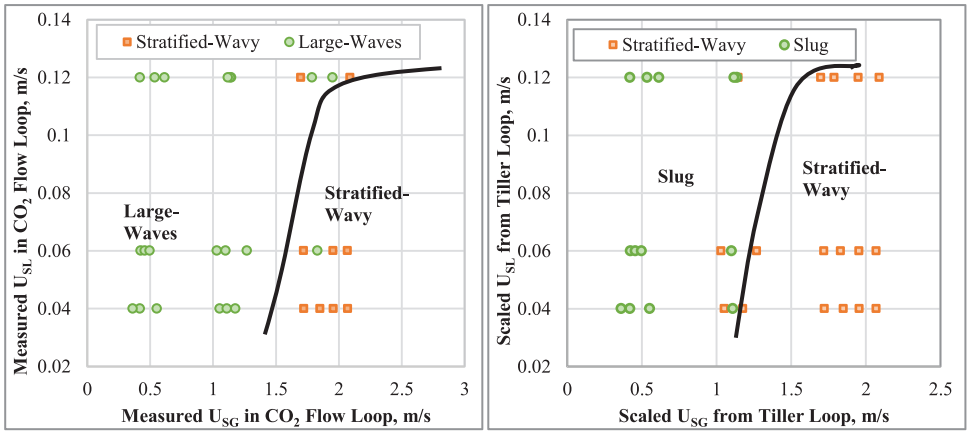

Fig. 11. Flow pattern map for CO_2 flow loop experiments (to the left) corresponding to Tiller dataset 2 (to the right).

10. Conclusion

In earlier studies at IFE, the concepts of geometric, kinematic, and dynamic similarities were used to select a set of eight dimensionless parameters to characterize two-phase pipe flow. The experiments that were designed to test the scale-up rules, gave a much better match with the corresponding experiments when the density ratio was matched. The work presented in this paper is carried out using the IFE CO_2 Flow Loop which allows matching of the density ratio to be improved significantly.

This work has focused on dimensional analysis and scaling rules for multiphase flow in fully-developed, steady-state, two-phase, gas–liquid, stratified and stratified-wavy flows. A total of 38 experimental subsets were conducted with pure CO_2 at different pressure/temperature combinations, all on the equilibrium line, and with a few different pipe inclinations. It is challenging to find a fluid system that matches all the similarity criteria, and we prioritized a system that has the correct density ratio. Total pressure gradients, liquid holdups and flow patterns were compared with scaled values from corresponding experiments at larger scales. The discrepancy between the new experimental results and the scaled data from previous experiments is generally very small and within the uncertainty of the data. The conclusion is that the scale-up approach works very well. These experiments confirm that the gas–liquid density ratio is a very important parameter of multiphase pipe flow. One should therefore be very cautious to use results from lab experiments directly to field applications, unless the gas–liquid density ratios are similar.

Moreover, we have observed discrepancies in the pressure gradients for high superficial gas velocities. We have used the Froude number to preserve dynamic similarity in hydraulic modelling of multiphase flows influenced by gravity. For high gas superficial velocity, there may be a lot of droplet entrainment and assuming similarity through the squared Froude number may not be fully adequate.

In closing, we have demonstrated that matching the gas–liquid density ratio, the pipe inclination, the Froude number, and the liquid-to-gas velocity ratio are sufficient to give very good scaling behaviour of experiments in two-phase stratified and stratified wavy flow, with excellent agreement even when scaling the diameter with a factor of 6.5. Values of liquid viscosities and gas–liquid interfacial tensions scaled down from the Tiller loop to the CO_2 loop deviate by factors of 0.8–4 and 5–10, respectively. Despite the significant differences in these two parameters, our results showed an excellent match with the Tiller datasets with the same density ratios, indicating that the surface tension and viscosity have little influence on the overall flow behaviour for these conditions.

Declaration of Competing Interest

The authors state that there are no interests to declare.

Acknowledgement

This work is part of the SUM project (**S**caling and **U**ncertainties in **M**ultiphase Flow), which is supported by the Norwegian Research Council and industrial partners from the SINTEF-IFE MULTIFLOW JIP (Schlumberger Information Solution, Equinor, Lundin Norway, LedaFlow Technologies DA, Gassco, ENI Norge and TechnipFMC). We would also like to thank SINTEF Industry and Equinor for making the data available.

Supplementary materials

Supplementary material associated with this article can be found, in the online version, at doi:10.1016/j.ijmultiphaseflow.2019.103139.

Appendix A

Table 6 and 7.

Table 6
Experimental results corresponding to Dataset 1.

Exp	U_{SG}	U_{SL}	|dp/dx|	H_L	Flow*	Exp	U_{SG}	U_{SL}	|dp/dx|	H_L	Flow	Exp	U_{SG}	U_{SL}	|dp/dx|	H_L	Flow
Exp	3.87	0.05	353	0.01	SA	Exp	5.03	0.05	466	0.02	SA	Exp	4.60	0.10	472	0.04	SA
1	1.88	0.05	100	0.05	SA	11	3.45	0.05	237	0.04	SA	20	3.66	0.10	318	0.06	SA
	0.51	0.05	17	0.18	SW		1.68	0.05	63	0.08	SW		1.66	0.10	109	0.16	SW
Exp	3.93	0.10	382	0.00	SA		0.44	0.05	8	0.20	SW		0.49	0.10	107	0.50	LW
2	2.06	0.10	126	0.05	SA	Exp	5.02	0.10	524	0.02	SA	Exp	4.55	0.50	824	0.13	LW
	0.53	0.10	24	0.27	SW	12	3.44	0.10	262	0.06	SA	21	3.58	0.50	606	0.20	LW
Exp	4.98	0.50	940	0.08	LW		1.68	0.10	74	0.12	SW		1.61	0.50	270	0.36	LW
3	3.94	0.50	692	0.09	LW		0.44	0.10	12	0.27	SW	Exp	4.61	0.03	420	0.01	SA
	0.52	0.50	92	0.52	LW	Exp	3.82	0.50	609	0.17	LW	22	3.45	0.03	239	0.02	SA
Exp	1.38	0.78	280	0.49	LW	13	2.12	0.50	270	0.29	LW		1.70	0.03	47	0.05	SW
4	0.50	0.78	156	0.70	LW		1.87	0.50	233	0.31	LW		0.90	0.03	−3.4	0.07	SW
Exp	4.92	0.10	511	0.03	SA		0.47	0.50	76	0.58	LW	Exp	3.47	0.05	270	0.01	SA
5	3.65	0.10	314	0.06	SA	Exp	4.68	0.03	485	0.02	SA	23	1.70	0.05	54	0.05	SW
	2.67	0.10	176	0.09	SW	14	3.74	0.03	327	0.03	SA		0.75	0.05	−6	0.08	SW
	1.17	0.10	48	0.19	SW		1.96	0.03	120	0.06	SA	Exp	4.67	0.10	508	0.01	SA
	0.55	0.10	21	0.32	SW		0.59	0.03	86	0.38	SW	24	3.48	0.10	301	0.03	SA
Exp	4.88	0.19	655	0.06	SA	Exp	4.65	0.05	481	0.02	SA		1.71	0.10	62	0.09	SW
6	3.63	0.19	392	0.08	SA	15	1.94	0.05	126	0.09	SA		0.75	0.10	−5	0.13	SW
	2.64	0.19	222	0.13	SW		1.67	0.05	104	0.10	SW		0.43	0.10	−14	0.12	SS
	1.16	0.19	71	0.24	SW		0.70	0.05	86	0.35	SW	Exp	4.16	0.50	708	0.13	LW
	0.51	0.19	32	0.42	SW	Exp	4.66	0.10	529	0.02	SA	25	3.43	0.50	515	0.19	LW
Exp	4.97	0.29	724	0.06	SA	16	3.94	0.10	414	0.03	SA		1.69	0.50	165	0.35	LW
7	3.65	0.29	449	0.12	SA		1.95	0.10	142	0.12	SA		0.78	0.50	29	0.47	LW
	2.42	0.29	232	0.19	SW		0.61	0.10	104	0.44	SW	Exp	3.63	0.03	204	0.02	SA
Exp	4.73	0.38	779	0.08	LW	Exp	4.47	0.50	840	0.10	AN	26	1.67	0.03	35	0.05	SW
8	3.10	0.38	407	0.18	LW	17	4.03	0.50	723	0.12	LW		0.25	0.03	−14	0.06	SW
	2.61	0.38	317	0.21	LW		2.09	0.50	327	0.30	LW	Exp	3.43	0.05	193	0.03	SA
	1.64	0.38	169	0.30	LW		0.63	0.50	179	0.59	LW	27	1.68	0.05	38	0.06	SW
	1.15	0.38	118	0.37	LW	Exp	4.47	0.03	354	0.02	SA		0.22	0.05	−15	0.09	SW
Exp	2.84	0.62	489	0.25	LW	18	3.52	0.03	232	0.03	SA	Exp	3.49	0.10	235	0.05	SA
9	2.11	0.62	346	0.33	LW		1.59	0.03	76	0.08	SW	28	1.67	0.10	44	0.11	SW
	1.86	0.62	302	0.35	LW		0.44	0.03	99	0.48	LW		0.23	0.10	−15	0.13	SW
	0.88	0.62	158	0.51	LW	Exp	4.62	0.05	404	0.01	SA	Exp	4.51	0.50	704	0.13	LW
Exp	5.36	0.03	467	0.00	SA	19	3.42	0.05	238	0.02	SA	29	3.33	0.50	438	0.19	LW
10	3.66	0.03	227	0.01	SA		1.66	0.05	86	0.07	SW		2.12	0.50	203	0.28	LW
	1.67	0.03	54	0.04	SW		0.58	0.05	93	0.38	LW		0.24	0.50	−19	0.45	SW

* SA is stratified-annular flow, SW is stratified-wavy flow and LW is large-waves flow.

Table 7
Experimental results corresponding to Dataset 2.

Exp	U_{SG}	U_{SL}	|dp/dx|	H_L	Flow	Exp	U_{SG}	U_{SL}	|dp/dx|	H_L	Flow	Exp	U_{SG}	U_{SL}	|dp/dx|	H_L	Flow
Exp	2.07	0.04	250	0.07	SW	Exp	4.16	0.04	400	0.04	SA	Exp	3.64	0.04	311	0.03	SA
30	1.72	0.04	239	0.10	SW	33	1.96	0.04	229	0.12	SW	36	1.85	0.04	228	0.12	SW
	1.18	0.04	265	0.18	LW		1.05	0.04	300	0.26	LW		1.11	0.04	303	0.24	LW
	0.42	0.04	481	0.54	LW		0.36	0.04	548	0.61	LW		0.55	0.04	456	0.47	LW
Exp	2.07	0.06	276	0.09	SW	Exp	4.14	0.06	435	0.04	SA	Exp	3.64		342	0.04	SA
31	1.72	0.06	264	0.12	SW	34	1.95	0.06	252	0.13	SW	37	1.83	0.06	251	0.14	LW
	1.27	0.06	276	0.19	LW		1.03	0.06	322	0.29	LW		1.10	0.06	328	0.27	LW
	0.42	0.06	490	0.51	LW		0.46	0.06	510	0.54	LW		0.50	0.06	501	0.52	LW
Exp	2.09	0.12	338	0.13	SW	Exp	4.12	0.12	540	0.07	SA	Exp	3.60	0.12	445	0.078	LW
32	1.70	0.12	322	0.17	SW	35	1.95	0.12	326	0.18	LW	38	1.79	0.12	318	0.19	LW
	1.14	0.12	338	0.27	LW		1.14	0.12	366	0.32	LW		1.12	0.12	385	0.33	LW
	0.42	0.12	513	0.58	LW		0.61	0.12	485	0.50	LW		0.54	0.12	528	0.54	LW

References

Abduvayt, P., Arihara, N., Manabe, A., Ikeda, K., 2003. Experimental and modeling studies for gas–liquid two-phase flow at high pressure conditions. J. Jpn. Pet. Inst. 46 (2), 111–125.

AlSarkhi, A., Duc, V., Sarica, C., Pereryra, E., 2016. Upscaling modeling using dimensional analysis in gas–liquid annular and stratified flows. J. Pet. Sci. Eng. 137, 240–249.

Alsarkhi, A., Sarica, C., Pereyra, E., 2016. New dimensionless number for gas–liquid flow in pipes. Int. J. Multiph. Flow 81, 15–19.

Buckingham, E., 1914. On physically similar systems: illustrations of the use of dimensional equations. Phys. Rev. 4, 345–376.

Hald, K., Lawrence, C., Sagen, J., 2013. Scale up SIS. Scale up SIS, 189 Kjeller: IFE internal report.

Hasan, A., Shah Kabir, C., Sayarpour, M., 2007. A Basic Approach to Wellbore Two-Phase Flow Modeling. Society of Petroleum Engineers, Anaheim, California.

Hedne, P., 1988. Experiments with naphtha. In: Experiments with naphtha, 11, p. F88053 Trondheim: SINTEF internal report STF.

Hedne, P., 1996. Large scale inclined pipe experiments. In: Large scale inclined pipe experiments, 84, p. F96053 Trondheim: SINTEF internal report STF.

Heggum, G., 1993. Inclined flow experiments with naphtha. In: Inclined flow experiments with naphtha, 11, p. F93013 Trondheim: SINTEF internal report STF.

Langhaar, H.L., 1951. Dimensional Analysis and the Theory of Models. Wiley, New York.

Lawrence, C., Hald, K., Langsholt, M., Liu, L., 2012. Scale up SIS. Scale up SIS, 102 Kjeller: IFE internal report.

Linga, H., Hedne, P., 1987. Experiments with naphtha, May–June 1987 Trondheim: SINTEF report STF11 FF87053.

Linga, H., Østvang, D., 1985. Experiments with naphtha. In: Experiments with naphtha, 11, p. F85005 Trondheim: SINTEF internal report STF.

Sharp, J., 1981. Hydraulic Modelling. Butterworths, London.

US Department of Commerce, n.d. National Institute of Standards and Technology. [Online] Available at: https://down.nist.gov.